STRUCTURAL CHEMISTRY

ISSN 2053-2296

Crystal, electronic structure and hydrogenation properties of the $Mg_{5.57}Ni_{16}Ge_{7.43}$ cluster phase with a new type of polyhedron

Nazar Pavlyuk,[a] Grygoriy Dmytriv,[a] Alina Bondaruk,[b] Wojciech Ciesielski[b] and Volodymyr Pavlyuk[a,b]*

[a]Department of Inorganic Chemistry, Ivan Franko Lviv National University, Kyryla and Mefodiya str. 6, 79005 Lviv, Ukraine, and [b]Institute of Chemistry, Jan Dlugosz University, al. Armii Krajowej 13/15, Czestochowa 42200, Poland. *Correspondence e-mail: vpavlyuk2002@yahoo.com

Received 7 March 2024
Accepted 11 April 2024

Edited by G. P. A. Yap, University of Delaware, USA

Keywords: crystal structure; electronic structure; clusters; convex polyhedra; intermetallics; hydride; ternary; germanide; hydrogenation.

CCDC reference: 2347669

Supporting information: this article has supporting information at journals.iucr.org/c

The ternary germanide $Mg_{5.57}Ni_{16}Ge_{7.43}$ (cubic, space group $Fm\bar{3}m$, $cF116$) belongs to the structural family based on the Th_6Mn_{23}-type. The Ge1 and Ge2 atoms fully occupy the 4*a* ($m\bar{3}m$ symmetry) and 24*d* (*m.mm*) sites, respectively. The Ni1 and Ni2 atoms both fully occupy two 32*f* sites (.3*m* symmetry). The Mg/Ge statistical mixture occupies the 24*e* site with 4*m.m* symmetry. The structure of the title compound contains a three-core-shell cluster. At (0,0,0), there is a Ge1 atom which is surrounded by eight Ni atoms at the vertices of a cube and consequently six Mg atoms at the vertices of an octahedron. These surrounded eight Ni and six Mg atoms form a $[Ge1Ni_8(Mg/Ge)_6]$ rhombic dodecahedron with a coordination number of 14. The $[GeNi_8(Mg/Ge)_6]$ rhombic dodecahedron is encapsulated within the $[Ni_{24}]$ rhombicuboctahedron, which is again encapsulated within an $[Ni_{32}(Mg/Ge)_{24}]$ pentacontatetrahedron; thus, the three-core-shell cluster $[GeNi_8(Mg/Ge)_6@Ni_{24}@Ni_{32}(Mg/Ge)_{24}]$ results. The pentacontatetrahedron is a new representative of Pavlyuk's polyhedra group based on pentagonal, tetragonal and trigonal faces. The dominance of the metallic type of bonding between atoms in the $Mg_{5.57}Ni_{16}Ge_{7.43}$ structure is confirmed by the results of the electronic structure calculations. The hydrogen sorption capacity of this intermetallic at 570 K reaches 0.70 wt% H_2.

1. Introduction

Magnesium alloys and intermetallics, in addition to their unique mechanical properties, show great potential for use in various types of energy storage systems. These are in particular as hydrogen sorption materials for storage systems and metal hydride batteries (Edalati *et al.*, 2018; Ouyang *et al.*, 2020; Hitam *et al.*, 2021). Binary alloys of magnesium with transition metals, such as Fe, Co, Ni, Zn and others, as well as ternary alloys with the additional involvement of *p*-elements, such as Al, Ga, Si, Ge, Sn, rare earth metals and others, have attracted special attention (Kalisvaart *et al.*, 2010; Zhang *et al.*, 2011; Pavlyuk *et al.*, 2012, 2022*a*; Shtender *et al.*, 2015). Due to the complexities of the synthesis of magnesium alloys and the complex nature of the physicochemical interaction of magnesium with other elements, ternary metallic systems are still not sufficiently studied. For example, study of the ternary Mg–Ni–Ge system began more than 60 years ago when the first results of analyzing the structures of $MgNi_{1.6}Ge_{0.4}$ and $Mg_6Ni_{16}Ge_7$ by the powder Debye–Scherrer method were reported (Teslyuk & Markiv, 1962). $MgNi_{1.6}Ge_{0.4}$ (cubic, $Fd\bar{3}m$, a = 6.911 Å) belongs to the cubic Laves phase with the $MgCu_2$ structure type. For $Mg_6Ni_{16}Ge_7$ (cubic, $Fm\bar{3}m$, a = 11.532 Å), the $Mg_6Cu_{16}Si_7$ structure type was proposed.

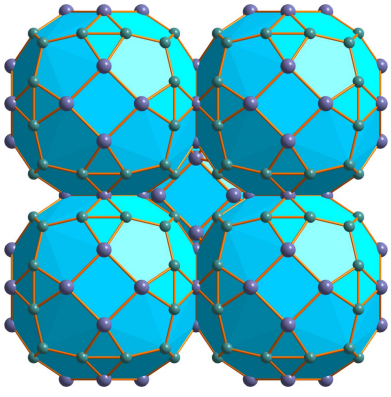

Buchholz & Schuster (1981) described the crystal structure of $MgNi_6Ge_6$ (hexagonal, *P*6/*mmm*, a = 5.067 and c = 3.860 Å) with the YCo_6Ge_6-type. The equiatomic MgNiGe phase (orthorhombic, *Pnma*, a = 6.4742, b = 4.0716 and c = 6.9426 Å) belongs to the TiNiSi-type (Hlukhyy *et al.*, 2013). The Mg-rich compound Mg_3Ni_2Ge (cubic, $Fd\bar{3}m$, a = 11.521 Å) crystallizes in the Mn_3Ni_2Si-type (Gennari *et al.*, 2003). Subsequently, the crystal structures of the two Laves phases Mg_2Ni_3Ge ($R\bar{3}m$, a = 5.0300 and c = 11.330 Å) and $MgNi_{2-x}Ge_x$ (x = 0.5, $P6_3/mcm$, a = 8.6946 and c = 7.8127 Å) were investigated using single-crystal X-ray diffraction methods (Siggelkow *et al.*, 2017).

During our investigation of Ni-rich alloys of the ternary Mg–Ni–Ge system, we obtained a good-quality single crystal of the $Mg_{5.57}Ni_{16}Ge_{7.43}$ ternary phase and report its crystal structure here.

2. Experimental

2.1. Synthesis and crystallization

The target $Mg_{20}Ni_{55}Ge_{25}$ species was prepared from the following reactants: magnesium, nickel and germanium (purity of elements is more than 99.99 wt%). Appropriate amounts of Mg, Ni and Ge pure elements were mixed according to the aimed-for stoichiometry of the product and filled into a tantalum crucible in a glove box using a purified argon atmosphere. The Ta crucible was sealed by arc welding under a dry argon atmosphere. The reaction between the elements was carried out in an induction furnace at 1100 °C. After 20 min, the samples were cooled rapidly to room temperature by removing the crucibles from the furnace. The Ta container was placed in an evacuated quartz vial and thermally annealed to obtain good-quality single crystals suitable for structure determination. This heating process was carried out at a rate of 5 °C min^{-1} to T = 800 °C in a resistance furnace and held at this temperature for 15–20 min with a thermal cycle controller. The sample was then cooled slowly (0.1 °C min^{-1}) to 400 °C and the furnace was switched off. After cooling to room temperature, the sample could be separated from the tantalum container. The alloy is stable in air and includes single crystals, which exhibit metallic luster and could be isolated by mechanical fragmentation.

2.2. Refinement

The structure was solved by direct methods after an analytical absorption correction.

The Mg atom in the 24*e* site showed a displacement parameter that was different from the others, *i.e.* the Ni and Ge atoms.

Several important factors indicate that the 24*e* position is occupied mainly by Mg atoms with a small fraction of germanium (a statistical mixture of Mg/Ge). First, the title compound is isostructural with the $Mg_6Cu_{16}Si_7$ structure type, where the 24*e* site is also occupied by Mg atoms. Second, analysis of the interatomic distances indicates that they are typical of the largest atom in this structure, which is magnesium. Thirdly, Fourier difference electron-density maps show the electron density to be associated with the Mg atom. During the first cycles of refinement of the Mg atom in the 24*e* site, we noticed that, in addition to magnesium, there is also a small proportion of the heavier Ge or Ni atom in this site. The best refinement results are for the Mg/Ge statistical mixture. The refined composition of the compound from single-crystal data correlates well with the energy-dispersive X-ray spectroscopy (EDS) analysis.

Table 1
Experimental details.

Crystal data	
Chemical formula	$Mg_{5.57}Ni_{16}Ge_{7.43}$
M_r	6454.98
Crystal system, space group	Cubic, $Fm\bar{3}m$
Temperature (K)	293
a (Å)	11.5036 (6)
V (Å^3)	1522.3 (2)
Z	1
Radiation type	Mo $K\alpha$
μ (mm^{-1})	33.86
Crystal size (mm)	0.06 × 0.05 × 0.03
Data collection	
Diffractometer	Oxford Diffraction Xcalibur3 CCD
Absorption correction	Analytical (*CrysAlis RED*; Oxford Diffraction, 2008)
T_{min}, T_{max}	0.470, 0.683
No. of measured, independent and observed [$I > 2\sigma(I)$] reflections	12619, 131, 120
R_{int}	0.074
(sin $\theta/\lambda)_{max}$ (Å^{-1})	0.668
Refinement	
$R[F^2 > 2\sigma(F^2)]$, $wR(F^2)$, S	0.013, 0.028, 1.25
No. of reflections	131
No. of parameters	14
$\Delta\rho_{max}$, $\Delta\rho_{min}$ (e Å^{-3})	0.63, −0.63

Computer programs: *CrysAlis PRO* (Rigaku OD, 2015), *SHELXT2014* (Sheldrick, 2015*a*), *SHELXL2014* (Sheldrick, 2015*b*), *DIAMOND* (Brandenburg, 2006) and *SHELX97* (Sheldrick, 1997).

Crystal data, data collection and structure refinement details are summarized in Table 1.

2.3. Hydrogenation

The hydrogen absorption and desorption measurements for the $Mg_{5.57}Ni_{16}Ge_{7.43}$ alloy were performed using an IMI–COR (Hiden Isochema) manometric hydrogen-storage analyzer. The Sieverts method, up to a pressure of 12 bar (1 bar = 10^5 Pa) at a temperature of 573 K, was used.

3. Results and discussion

As part of a systematic study of Mg–Ni–Ge alloys, the ternary $Mg_{5.57}Ni_{16}Ge_{7.43}$ phase was detected in the Ni-rich region. A small irregularly shaped single crystal was selected from the annealed sample by mechanical fragmentation. Intensity data were measured at room temperature on an Oxford Diffraction Xcalibur3 automatic diffractometer with a CCD detector (Mo $K\alpha$ radiation, graphite monochromator, ω scan).

The title compound crystallizes in a cubic $Mg_6Cu_{16}Si_7$ structure type (Nagorsen & Witte, 1953), which is an ordered

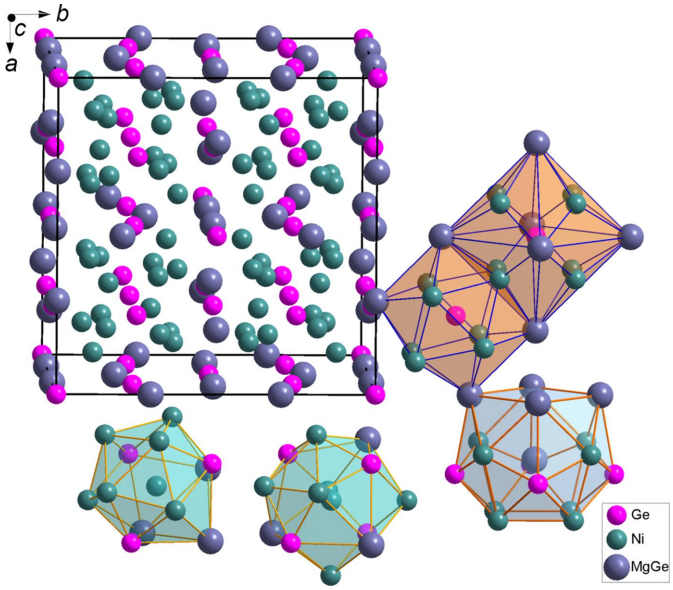

Figure 1
A clinographic projection of the $Mg_{5.57}Ni_{16}Ge_{7.43}$ unit-cell contents and the coordination polyhedra of the atoms.

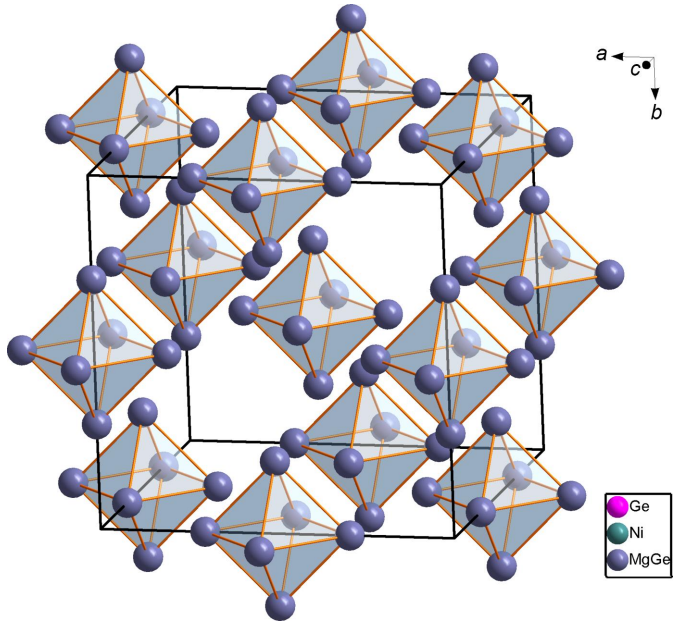

Figure 2
The packing of empty $[(Mg/Ge)_6]$ octahedra in the unit cell.

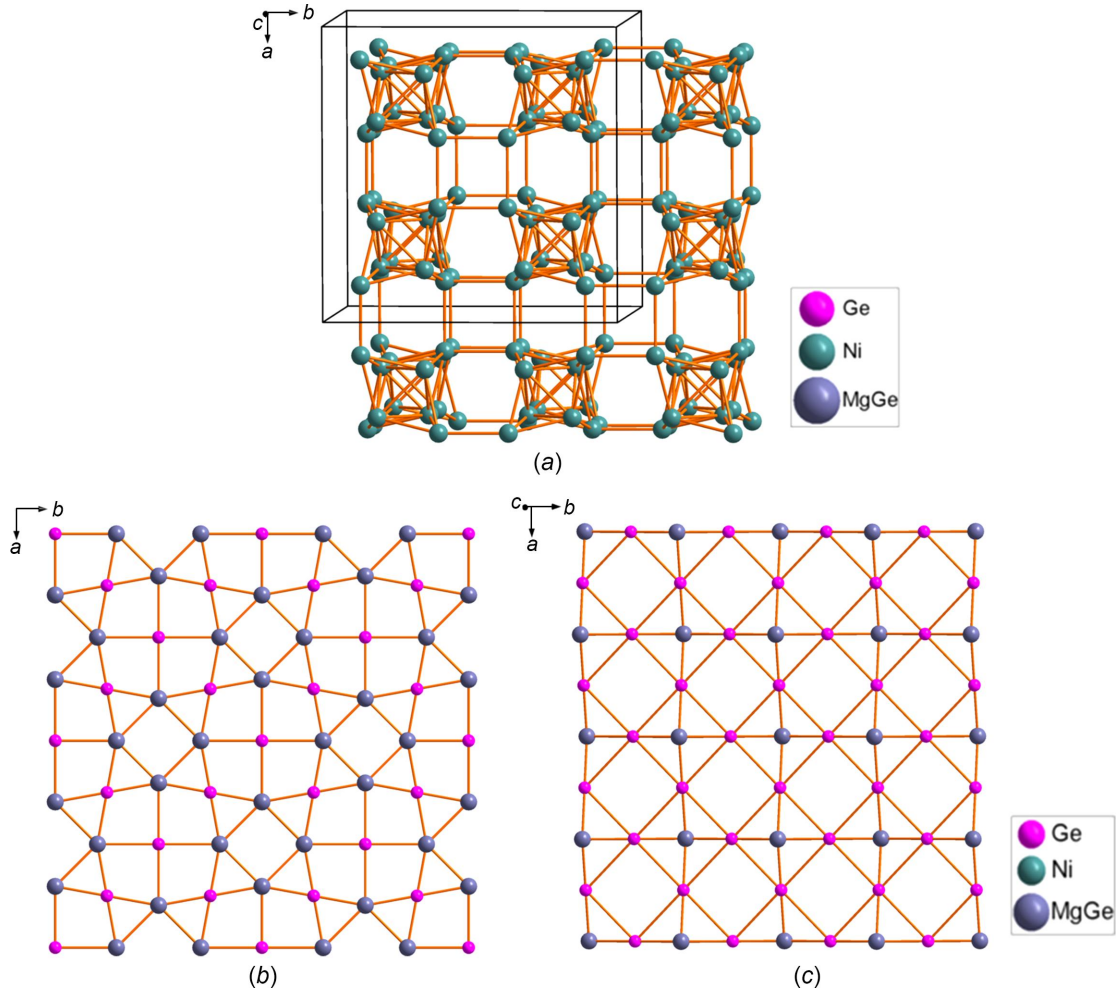

Figure 3
(*a*) Three-dimensional network of Ni atoms, (*b*) flat 3- and 4-ring networks of Mg–Ge atoms at $z = 0$ and $\frac{1}{2}$, and (*c*) slightly corrugated networks at $z = \frac{1}{4}$ and $\frac{3}{4}$ in the $Mg_{5.57}Ni_{16}Ge_{7.43}$ structure.

superstructure of the Th_6Mn_{23}-type (Florio *et al.*, 1952). The unit cell and coordination polyhedra of the crystallographically distinct atoms are shown in Fig. 1. The Mg/Ge atom (site symmetry 4*m.m*) is surrounded by 16 adjacent atoms, which form a pseudo-Frank–Kasper [(Mg/Ge)Ni_8(Mg/Ge)$_4$Ge$_4$] polyhedron. The coordination polyhedra of the Ni1 and Ni2 atoms (.3*m* symmetry) are icosahedral [Ni1Ge$_3$Ni$_6$-(Mg/Ge)$_3$] and pseudo-Frank–Kasper polyhedral (CN = 13) [Ni2Ge$_4$Ni$_6$(Mg/Ge)$_3$], respectively. At (0,0,0), there is a Ge1 atom surrounded by eight Ni atoms, which occupy the vertices of an [Ni_8] cube, and also by six Mg/Ge atoms, which are at the vertices of an [(Mg/Ge)$_6$] octahedron. The eight Ni atoms and six Mg/Ge atoms which surround the Ge1 atom form a [Ge1Ni_8(Mg/Ge)$_6$] rhombic dodecahedron with CN = 14. For the Ge2 atom, the polyhedron is a 14-vertex [Ge2Ni_8(Mg/Ge)$_6$] rhombododecahedron. In addition to octahedra filled by germanium, there are also empty [(Mg/Ge)$_6$] octahedra, the arrangement of which in the unit cell is shown in Fig. 2. Ni atoms form a three-dimensional network in which [Ni_8] cubes are visible, the vertices of which are joined by eight [Ni_4] tetrahedra, which are also connected to other tetrahedra by one face and three edges, as shown in Fig. 3(*a*). Instead, the Mg and Ge atoms along the *z* axis form two types of 3- and 4-ring networks, namely, flat at $z = 0$ and $\frac{1}{2}$ [Fig. 3(*b*)], and slightly corrugated at $z = \frac{1}{4}$ and $\frac{3}{4}$ [Fig. 3(*c*)].

The ternary germanide $Mg_{5.57}Ni_{16}Ge_{7.43}$ can also be described as three-core-shell clusters of [$GeNi_8$(Mg/Ge)$_6$@Ni_{24}@-Ni_{32}(Mg/Ge)$_{24}$] (see Fig. 4). The [$GeNi_8$(Mg/Ge)$_6$] rhombic dodecahedron is encapsulated within the [Ni_{24}] rhombicuboctahedron, which is again encapsulated within a [Ni_{32}(Mg/Ge)$_{24}$] pentacontatetrahedron. The [Ni_{32}(Mg/Ge)$_{24}$] polyhedron has vertices $V = 56$, faces $F = 54$ and edges $E = 108$. The Euler characteristic (χ) was classically defined for the surfaces of polyhedra, according to the formula (Richeson, 2012):

$$\chi = V - E + F,$$

where V, E and F are, respectively, the numbers of vertices (corners), edges and faces in the given polyhedron. For the title structure, the [Ni_{32}(Mg/Ge)$_{24}$] polyhedron has $V = 56$, $F = 54$ and $E = 108$, which gives a Euler characteristic χ of 2;

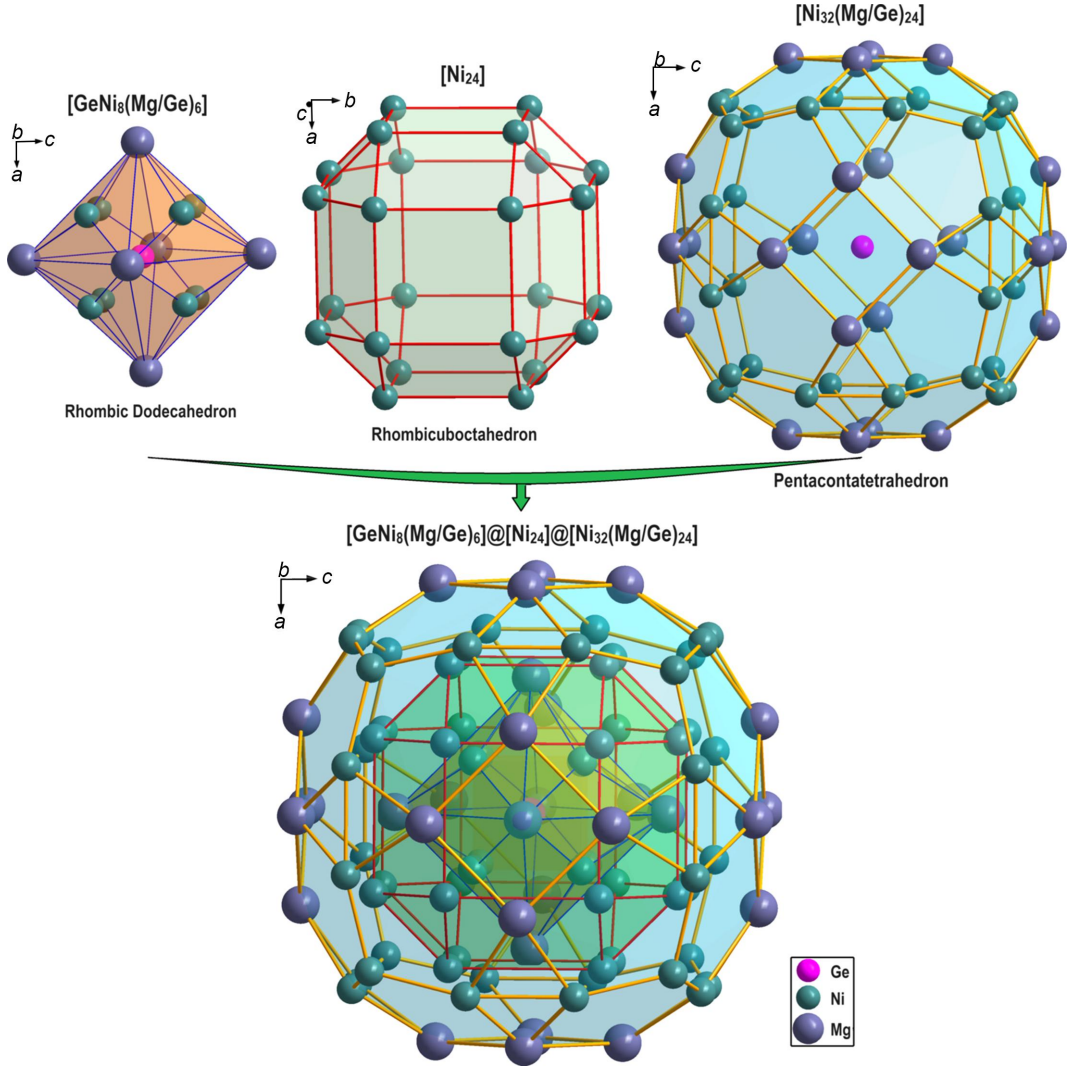

Figure 4
The atomic structure of a three-shell cluster [$GeNi_8$(Mg/Ge)$_6$@Ni_{24}@Ni_{32}(Mg/Ge)$_{24}$].

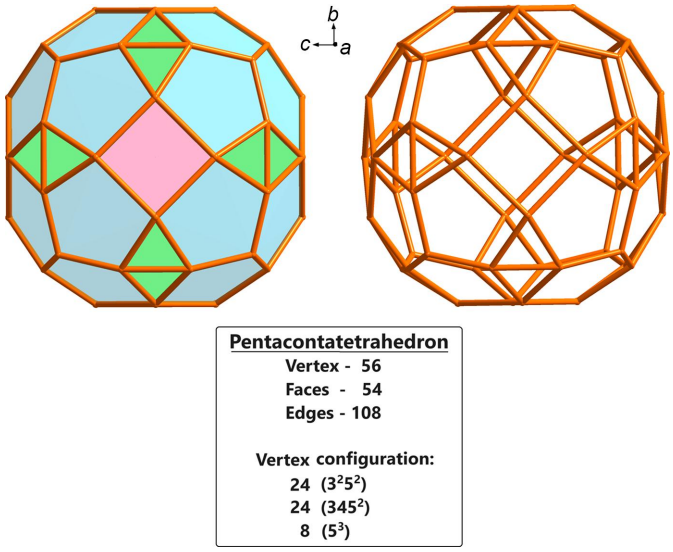

Figure 5
The closed and open faces of the $[Ni_{32}(Mg/Ge)_{24}]$ pentacontatetrahedron.

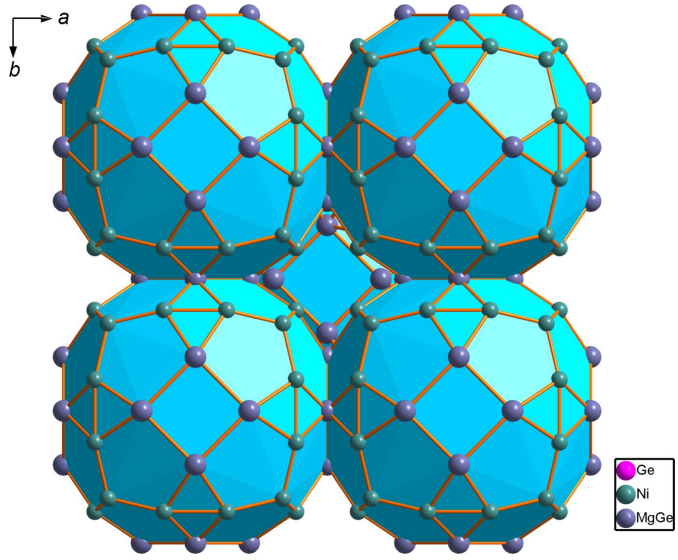

Figure 6
The packing of $[Ni_{32}(Mg/Ge)_{24}]$ pentacontatetrahedra in the unit cell.

therefore, $[Ni_{32}(Mg/Ge)_{24}]$ is a new type of convex polyhedron, namely, a pentacontatetrahedron, with the vertex configuration: 24 (3_25_2), 24 (345_2) and 8 (5_3). The pentacontatetrahedron is a new representative of Pavlyuk's group of polyhedra based on pentagonal, tetragonal and trigonal faces. In the pentacontatetrahedron are 24 pentagonal, six

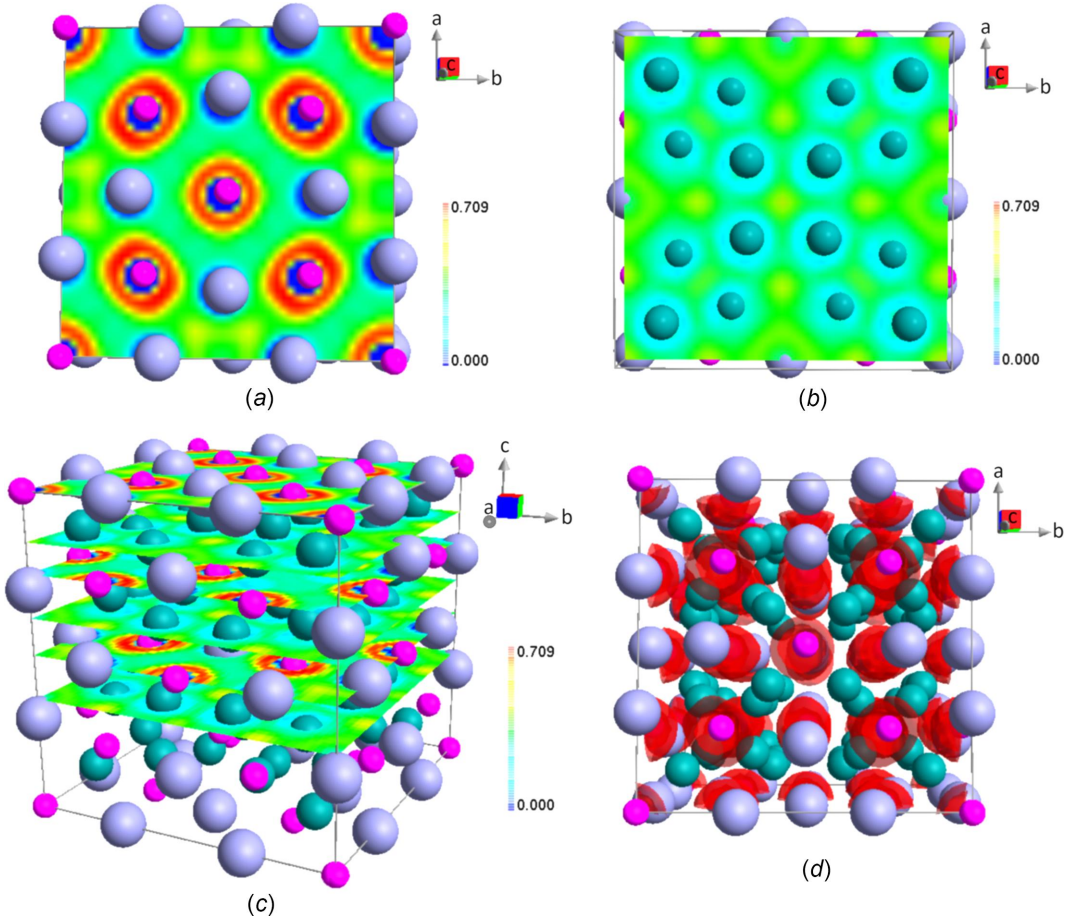

Figure 7
Two-dimensional representation of the ELF for layers of atoms at (*a*) $z = 0$ and (*b*) $z = \frac{1}{8}$. (*c*) Packing layers along the z axis and (*d*) a three-dimensional representation of the isosurfaces of the ELF around the Ge atoms at the 0.75 level.

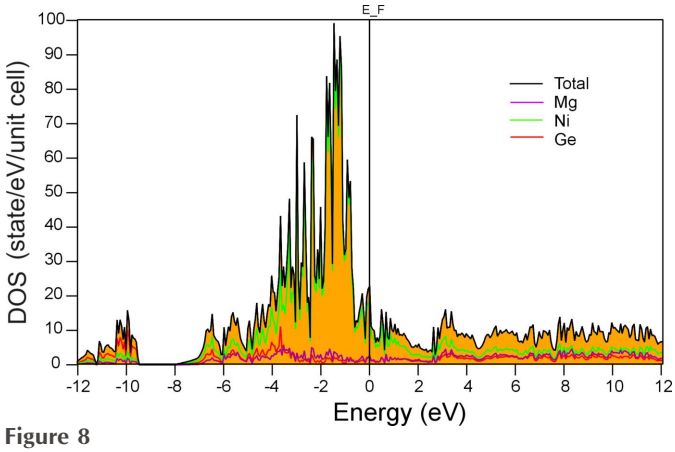

Figure 8
Total and partial DOS for $Mg_{5.57}Ni_{16}Ge_{7.43}$ from TB–LMTO–ASA calculations.

tetragonal and 24 trigonal faces (Fig. 5). In the title compound, the pentacontatetrahedra exhibits close packing in the unit cell (Fig. 6). Earlier, we described the structure of the cluster phase $MgMn_4Ga_{18}$ (Pavlyuk *et al.*, 2022*b*), for which we discovered a pentacontaoctahedron with $V = 40$, $F = 58$ and $E = 96$, and also a convex polyhedron ($\chi = 2$). We also described previously the formation of clusters in magnesium-containing intermetallics using the example of the quaternary phase $Li_{20}Mg_6Cu_{13}Al_{42}$ with a 60-atom truncated icosahedron (Pavlyuk *et al.*, 2019) and new cubic cluster phases in the Mg–Ni–Ga system (Pavlyuk *et al.*, 2020).

The electronic structure calculations were performed for the ordered structure $Mg_6Ni_{16}Ge_7$ (the 24*e* site is fully occupied by Mg) using the tight-binding linear muffin-tin orbital (TB–LMTO) method with the atomic spheres approximation (ASA) in the *TB–LMTO–ASA* program (Version 4.7; Andersen, 1975; Andersen *et al.*, 1984, 1986). Electronic energies were calculated using density functional theory (DFT) based on the local-density approximation (LDA) for the exchange-correlation functional as parameterized by von Barth & Hedin (1972). The electronic structure calculations were carried out using the non-spin-polarized approach with a dense k-point mesh in the irreducible Brillouin zones of the crystallographic unit cell (48 irreducible k-points from 512 for NKABC = 8 × 8 × 8). From the calculations, a mapping of the electrons in real space was obtained using the electron localization function (ELF) (Becke & Edgecombe, 1990). Visualization of the electronic structure calculation data was achieved using *wxDragon* (Eck, 2012). The ELF is a simple measure of electron localization in atomic and molecular systems (Becke & Edgecombe, 1990).

If we consider the distribution of the ELF, two types of layers of atoms can be distinguished in the title structure [Figs. 7(*a*) and 7(*b*)] which are alternately packed along the *z* axis [Fig. 7(*c*)]. Layers of atoms at $z = 0, \frac{1}{4}, \frac{1}{2}, \frac{3}{4}$ [Figs. 7(*a*) and 7(*c*)] consist exclusively of Mg and Ge atoms. The ELF has the highest values (0.709 eV) around the Ge atoms, which is consistent with its higher electronegativity [Figs. 7(*a*) and 7(*d*)]. Slightly corrugated layers of atoms at approximately $z = \frac{1}{8}, \frac{1}{3}, \frac{2}{3}$ and $\frac{7}{8}$ [Figs. 7(*a*) and 7(*c*)] consist exclusively of Ni atoms. The entire space of this layer has an average value of the distribution of the ELF function of 0.350 eV (indicated in green), which corresponds to delocalized electrons, which are typical for the metallic type of bonding between atoms. The dominance of the metallic bond is also reflected in the density of states (DOS) at the Fermi level, the partial and total DOS are shown in Fig. 8.

The prepared $Mg_{5.57}Ni_{16}Ge_{7.43}$ sample was hydrogenated by hydrogen gas at a pressure up to 12 bar and a temperature of 573 K. The PCT (pressure, composition and temperature) isotherms for the hydrogenation and dehydrogenation processes are presented in Fig. 9. At this condition, $Mg_{5.57}Ni_{16}Ge_{7.43}$ absorbs up to 0.7 wt% H_2. Crystallographic analysis of the structure made it possible to determine the geometrically acceptable coordinates of the sites that can be occupied by hydrogen, namely, 4*b* ($\frac{1}{2}, \frac{1}{2}, \frac{1}{2}$) and 48*h* ($\frac{1}{8}, \frac{1}{8}, 0$). These coordinates are the centres of the octahedral voids. In the 4*b* site, there is an $[(Mg/Ge)_6]$ octahedron, and in the 48*h* site, there is an octahedron of composition $[(Mg/Ge)_2Ni_2Ge_2]$, which is slightly deformed. In the case of full occupation of these sites with hydrogen, the hydrogen capacity reached 0.81 wt% H_2. A slight difference in the hydrogen content in hydride from experimental data and that calculated from geometric considerations indicates that these positions are partially occupied by H atoms (approximately 86%).

The bulk alloy from which the single crystal was selected was examined by scanning electron microscopy (SEM), energy dispersive X-ray spectroscopy (EDS) and powder X-ray diffraction (PXRD). A scanning electron microscope (TESCAN Vega3 LMU) equipped with an Oxford Instruments energy-dispersive X-ray analyzer (Aztec ONE system) was used to determine the chemical composition of the alloy (Fig. 10). The EDS data from three selected spots give the average composition (in at%) of $Mg_{19.3\,(3)}Ni_{55.2\,(2)}Ge_{25.5\,(1)}$ that correlates well with the PXRD data ($Mg_{19.21}Ni_{55.17}Ge_{25.62}$).

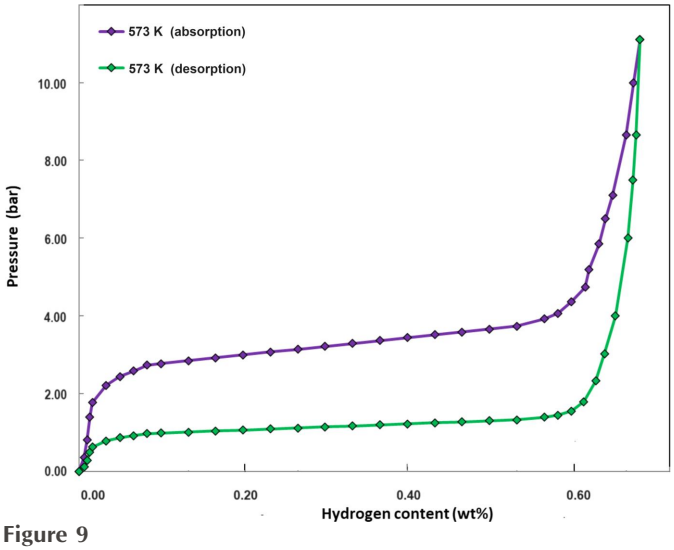

Figure 9
The PCT (pressure, composition and temperature) isotherms for hydrogenation and dehydrogenation processes.

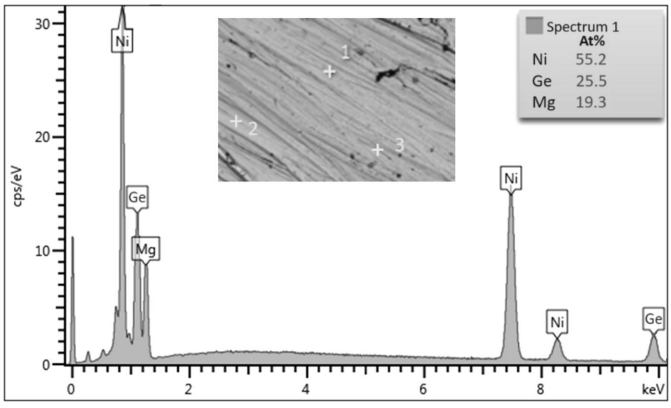

Figure 10
The secondary electron image and representative EDS spectra for the $Mg_{5.57}Ni_{16}Ge_{7.43}$ sample.

The PXRD analysis of the sample before and after hydrogenation was carried out using a Rigaku Mini Flex D-600 powder diffractometer with Cu $K\alpha$ radiation. As shown in Fig. 11, the structure of the intermetallic is preserved, and the shift of reflexes for the pattern after hydrogenation indicates an increase of the unit-cell dimension of the crystal lattice from a = 11.5036 (6) Å to a = 11.5753 (6) Å during the incorporation of hydrogen into the structural voids.

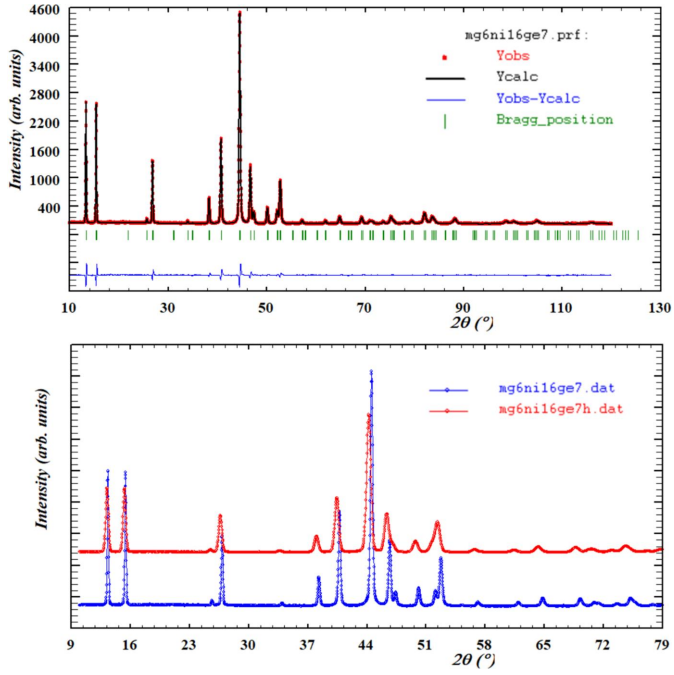

Figure 11
(*a*) Observed (red), calculated (black line) and difference (bottom blue line) PXRD patterns of the $Mg_{5.57}Ni_{16}Ge_{7.43}$ sample after Rietveld refinement. (*b*) Comparison powder patterns before (blue) and after (red) hydrogenation.

Funding information

Funding for this research was provided by: National Research Foundation of Ukraine (grant No. 2022.01/0064).

References

Andersen, O. K. (1975). *Phys. Rev. B*, **12**, 3060–3083.
Andersen, O. K. & Jepsen, O. (1984). *Phys. Rev. Lett.* **53**, 2571–2574.
Andersen, O. K., Pawlowska, Z. & Jepsen, O. (1986). *Phys. Rev. B*, **34**, 5253–5269.
Barth, U. & Hedin, L. (1972). *J. Phys. C.: Solid State Phys.* **5**, 1629–1642.
Becke, A. D. & Edgecombe, K. E. (1990). *J. Chem. Phys.* **92**, 5397–5403.
Brandenburg, K. (2006). *DIAMOND*. Version 3.1e. Crystal Impact GbR, Bonn, Germany.
Buchholz, W. & Schuster, H. U. (1981). *Z. Anorg. Allg. Chem.* **482**, 40–48.
Eck, B. (2012). *wxDragon*. Version 1.6.6. RWTH Aachen, Germany. http://schmeling.ac.rwth-aachen.de/cohp/download/wxDragon_Windows.zip.
Edalati, K., Uehiro, R., Ikeda, Y., Li, H. W., Emami, H., Filinchuk, Y., Arita, M., Sauvage, X., Tanaka, I., Akiba, E. & Horita, Z. (2018). *Acta Mater.* **149**, 88–96.
Florio, J. V., Rundle, R. E. & Snow, A. I. (1952). *Acta Cryst.* **5**, 449–457.
Gennari, F. C., Urretavizcaya, G., Andrade Gamboa, J. J. & Meyer, G. (2003). *J. Alloys Compd.* **354**, 187–192.
Hitam, C. N. C., Aziz, M. A. A., Ruhaimi, A. H. & Taib, M. R. (2021). *Int. J. Hydrogen Energy*, **46**, 31067–31083.
Hlukhyy, V., Hoffmann, A. V. & Fässler, T. F. (2013). *J. Solid State Chem.* **203**, 232–239.
Kalisvaart, W. P., Harrower, C. T., Haagsma, J., Zahiri, B., Luber, E. J., Ophus, C., Poirier, E., Fritzsche, H. & Mitlin, D. (2010). *Int. J. Hydrogen Energy*, **35**, 2091–2103.
Nagorsen, G. & Witte, H. (1953). *Z. Anorg. Allg. Chem.* **271**, 144–149.
Ouyang, L., Liu, F., Wang, H., Liu, J., Yang, X. S., Sun, L. & Zhu, M. (2020). *J. Alloys Compd.* **832**, 154865.
Oxford Diffraction (2008). *CrysAlis RED*. Oxford Diffraction Ltd, Abingdon, Oxfordshire, England.
Pavlyuk, N., Dmytriv, G., Pavlyuk, V., Chumak, I., Indris, S. & Ehrenberg, H. (2022*a*). *J. Phase Equilib. Diffus.* **43**, 458–470.
Pavlyuk, N., Dmytriv, G., Pavlyuk, V., Chumak, I., Indris, S., Schwarz, B. & Ehrenberg, H. (2022*b*). *Acta Cryst.* C**78**, 455–461.
Pavlyuk, N., Dmytriv, G., Pavlyuk, V. & Ehrenberg, H. (2019). *Acta Cryst.* B**75**, 168–174.
Pavlyuk, N., Dmytriv, G., Pavlyuk, V., Rozdzynska-Kielbik, B., Cichowicz, G., Cyranski, M. K., Chumak, I. & Ehrenberg, H. (2020). *Acta Cryst.* B**76**, 534–542.
Pavlyuk, V., Marciniak, B. & Różycka-Sokołowska, E. (2012). *Intermetallics*, **20**, 8–15.
Richeson, D. S. (2012). In *Euler's gem: the polyhedron formula and the birth of topology*. Princeton University Press.
Rigaku OD (2015). *CrysAlis PRO*. Rigaku Oxford Diffraction Ltd, Yarnton, Oxfordshire, England.
Sheldrick, G. M. (1997). *SHELXL97*. University of Göttingen, Germany.
Sheldrick, G. M. (2015*a*). *Acta Cryst.* A**71**, 3–8.
Sheldrick, G. M. (2015*b*). *Acta Cryst.* C**71**, 3–8.
Shtender, V. V., Denys, R. V., Zavaliy, I. Y., Zelinska, O. Y., Paul-Boncour, V. & Pavlyuk, V. V. (2015). *J. Solid State Chem.* **232**, 228–235.
Siggelkow, L., Hlukhyy, V. & Fässler, T. F. (2017). *Z. Anorg. Allg. Chem.* **643**, 1424–1430.
Teslyuk, M. Y. & Markiv, V. Y. (1962). *Sov. Phys. Crystallogr.* **7**, 103–104.
Zhang, Y. H., Li, B. W., Ren, H. P., Li, X., Qi, Y. & Zhao, D. L. (2011). *Materials*, **4**, 274–287.

supporting information

Acta Cryst. (2024). C**80**, 159-165 [https://doi.org/10.1107/S2053229624003140]

Crystal, electronic structure and hydrogenation properties of the $Mg_{5.57}Ni_{16}Ge_{7.43}$ cluster phase with a new type of polyhedron

Nazar Pavlyuk, Grygoriy Dmytriv, Alina Bondaruk, Wojciech Ciesielski and Volodymyr Pavlyuk

Computing details

Magnesium nickel germanide

Crystal data

$Mg_{5.57}Ni_{16}Ge_{7.43}$
M_r = 6454.98
Cubic, $Fm\bar{3}m$
a = 11.5036 (6) Å
V = 1522.3 (2) Å^3
Z = 1
$F(000)$ = 3010.1
D_x = 7.041 Mg m^{-3}
Mo $K\alpha$ radiation, λ = 0.71073 Å
Cell parameters from 131 reflections
θ = 3.1–28.3°
μ = 33.85 mm^{-1}
T = 293 K
Prism, metallic light grey
0.06 × 0.05 × 0.03 mm

Data collection

Oxford Diffraction Xcalibur3 CCD diffractometer
Radiation source: fine-focus sealed tube
ω scans
Absorption correction: analytical (CrysAlis RED; Oxford Diffraction, 2008)
T_{min} = 0.470, T_{max} = 0.683
12619 measured reflections
131 independent reflections
120 reflections with $I > 2\sigma(I)$
R_{int} = 0.074
θ_{max} = 28.3°, θ_{min} = 3.1°
h = −15→15
k = −15→15
l = −15→15

Refinement

Refinement on F^2
Least-squares matrix: full
$R[F^2 > 2\sigma(F^2)]$ = 0.013
$wR(F^2)$ = 0.028
S = 1.25
131 reflections
14 parameters
0 restraints
$w = 1/[\sigma^2(F_o^2) + 35.3811P]$ where $P = (F_o^2 + 2F_c^2)/3$
$(\Delta/\sigma)_{max} < 0.001$
$\Delta\rho_{max}$ = 0.63 e Å^{-3}
$\Delta\rho_{min}$ = −0.63 e Å^{-3}

Special details

Geometry. All esds (except the esd in the dihedral angle between two l.s. planes) are estimated using the full covariance matrix. The cell esds are taken into account individually in the estimation of esds in distances, angles and torsion angles; correlations between esds in cell parameters are only used when they are defined by crystal symmetry. An approximate (isotropic) treatment of cell esds is used for estimating esds involving l.s. planes.

Fractional atomic coordinates and isotropic or equivalent isotropic displacement parameters (Å²)

	x	*y*	*z*	U_{iso}*/U_{eq}	Occ. (<1)
Ge1	0.0000	0.0000	0.0000	0.0040 (4)	
Ge2	0.0000	0.2500	0.2500	0.00442 (18)	
Ni1	0.33129 (4)	0.33129 (4)	0.33129 (4)	0.00491 (19)	
Ni2	0.11860 (4)	0.11860 (4)	0.11860 (4)	0.00509 (19)	
Mg	0.2959 (2)	0.0000	0.0000	0.0048 (4)	0.929 (4)
Ge	0.2959 (2)	0.0000	0.0000	0.0048 (4)	0.071 (4)

Atomic displacement parameters (Å²)

	U^{11}	U^{22}	U^{33}	U^{12}	U^{13}	U^{23}
Ge1	0.0040 (4)	0.0040 (4)	0.0040 (4)	0.000	0.000	0.000
Ge2	0.0039 (4)	0.0047 (2)	0.0047 (2)	0.000	0.000	0.0002 (3)
Ni1	0.00491 (19)	0.00491 (19)	0.00491 (19)	0.00057 (18)	0.00057 (18)	0.00057 (18)
Ni2	0.00509 (19)	0.00509 (19)	0.00509 (19)	−0.00015 (18)	−0.00015 (18)	−0.00015 (18)
Mg	0.0073 (10)	0.0035 (6)	0.0035 (6)	0.000	0.000	0.000
Ge	0.0073 (10)	0.0035 (6)	0.0035 (6)	0.000	0.000	0.000

Geometric parameters (Å, º)

Ge1—Ni2	2.3631 (8)	Ni1—Ni1^{x}	2.6450 (14)
Ge1—Ni2^{i}	2.3632 (8)	Ni1—Ni1^{xii}	2.6450 (14)
Ge1—Ni2^{ii}	2.3632 (8)	Ni1—Ge^{xx}	2.7747 (7)
Ge1—Ni2^{iii}	2.3632 (8)	Ni1—Mg^{xxi}	2.7747 (7)
Ge1—Ni2^{iv}	2.3632 (8)	Ni1—Mg^{xxii}	2.7747 (7)
Ge1—Ni2^{v}	2.3632 (8)	Ni2—Ge2^{xvii}	2.5359 (3)
Ge1—Ni2^{vi}	2.3632 (8)	Ni2—Ge2^{xv}	2.5359 (3)
Ge1—Ni2^{vii}	2.3632 (8)	Ni2—Ni1^{ix}	2.5789 (7)
Ge2—Ni1^{viii}	2.3485 (1)	Ni2—Ni1^{xii}	2.5789 (7)
Ge2—Ni1^{ix}	2.3485 (1)	Ni2—Ni1^{x}	2.5789 (7)
Ge2—Ni1^{x}	2.3485 (1)	Ni2—Ni2^{ii}	2.7288 (9)
Ge2—Ni1^{xi}	2.3485 (1)	Ni2—Ni2^{vi}	2.7288 (9)
Ge2—Ni2^{ii}	2.5359 (3)	Ni2—Ni2^{iv}	2.7288 (9)
Ge2—Ni2^{xii}	2.5359 (3)	Ni2—Ge^{xvii}	2.8075 (17)
Ge2—Ni2^{xiii}	2.5359 (3)	Ni2—Ge^{xv}	2.8075 (17)
Ge2—Ni2	2.5359 (3)	Mg—Ni1^{xii}	2.7747 (7)
Ge2—Ge^{xiv}	2.9239 (4)	Mg—Ni1^{xxiii}	2.7747 (7)
Ge2—Mg^{xv}	2.9239 (4)	Mg—Ni1^{xxiv}	2.7747 (7)
Ge2—Mg^{xvi}	2.9239 (4)	Mg—Ni1^{xxv}	2.7747 (7)
Ge2—Mg^{xvii}	2.9239 (4)	Mg—Ni2^{vii}	2.8075 (17)
Ni1—Ge2^{xviii}	2.3485 (1)	Mg—Ni2^{vi}	2.8075 (17)
Ni1—Ge2^{x}	2.3485 (1)	Mg—Ni2^{iv}	2.8075 (17)
Ni1—Ge2^{xix}	2.3485 (1)	Mg—Ge2^{xxvi}	2.9239 (4)
Ni1—Ni2^{x}	2.5788 (7)	Mg—Ge2^{xxvii}	2.9239 (4)
Ni1—Ni2^{xii}	2.5788 (7)	Mg—Ge2^{xv}	2.9239 (4)
Ni1—Ni2^{ix}	2.5788 (7)	Mg—Ge2^{xvii}	2.9239 (4)

Ni1—Ni1^{ix}	2.6450 (14)		
Ni2—Ge1—Ni2^{i}	180.00 (4)	Ni1^{x}—Ni1—Mg^{xxi}	113.00 (4)
Ni2—Ge1—Ni2^{ii}	70.5	Ni1^{xii}—Ni1—Mg^{xxi}	171.56 (5)
Ni2^{i}—Ge1—Ni2^{ii}	109.5	Ge^{xx}—Ni1—Mg^{xxi}	73.5
Ni2—Ge1—Ni2^{iii}	109.5	Ge2^{xviii}—Ni1—Mg^{xxii}	69.03 (2)
Ni2^{i}—Ge1—Ni2^{iii}	70.5	Ge2^{x}—Ni1—Mg^{xxii}	69.03 (2)
Ni2^{ii}—Ge1—Ni2^{iii}	70.5	Ge2^{xix}—Ni1—Mg^{xxii}	132.71 (6)
Ni2—Ge1—Ni2^{iv}	70.5	Ni2^{x}—Ni1—Mg^{xxii}	122.689 (18)
Ni2^{i}—Ge1—Ni2^{iv}	109.5	Ni2^{xii}—Ni1—Mg^{xxii}	122.689 (18)
Ni2^{ii}—Ge1—Ni2^{iv}	109.5	Ni2^{ix}—Ni1—Mg^{xxii}	63.13 (5)
Ni2^{iii}—Ge1—Ni2^{iv}	180.00 (6)	Ni1^{ix}—Ni1—Mg^{xxii}	171.56 (5)
Ni2—Ge1—Ni2^{v}	109.5	Ni1^{x}—Ni1—Mg^{xxii}	113.00 (4)
Ni2^{i}—Ge1—Ni2^{v}	70.529 (1)	Ni1^{xii}—Ni1—Mg^{xxii}	113.00 (4)
Ni2^{ii}—Ge1—Ni2^{v}	70.5	Ge^{xx}—Ni1—Mg^{xxii}	73.5
Ni2^{iii}—Ge1—Ni2^{v}	109.5	Mg^{xxi}—Ni1—Mg^{xxii}	73.51 (7)
Ni2^{iv}—Ge1—Ni2^{v}	70.5	Ge1—Ni2—Ge2^{xvii}	112.187 (17)
Ni2—Ge1—Ni2^{vi}	70.5	Ge1—Ni2—Ge2	112.187 (17)
Ni2^{i}—Ge1—Ni2^{vi}	109.5	Ge2^{xvii}—Ni2—Ge2	106.624 (19)
Ni2^{ii}—Ge1—Ni2^{vi}	109.5	Ge1—Ni2—Ge2^{xv}	112.187 (17)
Ni2^{iii}—Ge1—Ni2^{vi}	70.5	Ge2^{xvii}—Ni2—Ge2^{xv}	106.624 (19)
Ni2^{iv}—Ge1—Ni2^{vi}	109.5	Ge2—Ni2—Ge2^{xv}	106.624 (19)
Ni2^{v}—Ge1—Ni2^{vi}	180.00 (6)	Ge1—Ni2—Ni1^{ix}	143.69 (2)
Ni2—Ge1—Ni2^{vii}	109.5	Ge2^{xvii}—Ni2—Ni1^{ix}	54.658 (12)
Ni2^{i}—Ge1—Ni2^{vii}	70.5	Ge2—Ni2—Ni1^{ix}	54.658 (12)
Ni2^{ii}—Ge1—Ni2^{vii}	180.00 (4)	Ge2^{xv}—Ni2—Ni1^{ix}	104.12 (3)
Ni2^{iii}—Ge1—Ni2^{vii}	109.5	Ge1—Ni2—Ni1^{xii}	143.69 (2)
Ni2^{iv}—Ge1—Ni2^{vii}	70.5	Ge2^{xvii}—Ni2—Ni1^{xii}	54.658 (12)
Ni2^{v}—Ge1—Ni2^{vii}	109.5	Ge2—Ni2—Ni1^{xii}	104.12 (3)
Ni2^{vi}—Ge1—Ni2^{vii}	70.5	Ge2^{xv}—Ni2—Ni1^{xii}	54.658 (12)
Ni1^{viii}—Ge2—Ni1^{ix}	180.0	Ni1^{ix}—Ni2—Ni1^{xii}	61.70 (3)
Ni1^{viii}—Ge2—Ni1^{x}	111.46 (4)	Ge1—Ni2—Ni1^{x}	143.69 (2)
Ni1^{ix}—Ge2—Ni1^{x}	68.54 (4)	Ge2^{xvii}—Ni2—Ni1^{x}	104.12 (3)
Ni1^{viii}—Ge2—Ni1^{xi}	68.54 (4)	Ge2—Ni2—Ni1^{x}	54.658 (12)
Ni1^{ix}—Ge2—Ni1^{xi}	111.46 (4)	Ge2^{xv}—Ni2—Ni1^{x}	54.658 (12)
Ni1^{x}—Ge2—Ni1^{xi}	180.0	Ni1^{ix}—Ni2—Ni1^{x}	61.70 (3)
Ni1^{viii}—Ge2—Ni2^{ii}	63.601 (15)	Ni1^{xii}—Ni2—Ni1^{x}	61.70 (3)
Ni1^{ix}—Ge2—Ni2^{ii}	116.399 (15)	Ge1—Ni2—Ni2^{ii}	54.7
Ni1^{x}—Ge2—Ni2^{ii}	116.399 (15)	Ge2^{xvii}—Ni2—Ni2^{ii}	126.587 (8)
Ni1^{xi}—Ge2—Ni2^{ii}	63.601 (15)	Ge2—Ni2—Ni2^{ii}	57.451 (17)
Ni1^{viii}—Ge2—Ni2^{xii}	116.399 (15)	Ge2^{xv}—Ni2—Ni2^{ii}	126.587 (8)
Ni1^{ix}—Ge2—Ni2^{xii}	63.601 (15)	Ni1^{ix}—Ni2—Ni2^{ii}	102.914 (14)
Ni1^{x}—Ge2—Ni2^{xii}	63.601 (15)	Ni1^{xii}—Ni2—Ni2^{ii}	161.57 (2)
Ni1^{xi}—Ge2—Ni2^{xii}	116.399 (15)	Ni1^{x}—Ni2—Ni2^{ii}	102.914 (14)
Ni2^{ii}—Ge2—Ni2^{xii}	180.00 (3)	Ge1—Ni2—Ni2^{vi}	54.7
Ni1^{viii}—Ge2—Ni2^{xiii}	63.601 (15)	Ge2^{xvii}—Ni2—Ni2^{vi}	126.587 (8)
Ni1^{ix}—Ge2—Ni2^{xiii}	116.399 (15)	Ge2—Ni2—Ni2^{vi}	126.587 (8)
Ni1^{x}—Ge2—Ni2^{xiii}	116.399 (15)	Ge2^{xv}—Ni2—Ni2^{vi}	57.451 (17)

Ni1^{xi}—Ge2—Ni2^{xiii}	63.601 (15)	Ni1^{ix}—Ni2—Ni2^{vi}	161.57 (2)
Ni2^{ii}—Ge2—Ni2^{xiii}	114.90 (3)	Ni1^{xii}—Ni2—Ni2^{vi}	102.914 (14)
Ni2^{xii}—Ge2—Ni2^{xiii}	65.10 (3)	Ni1^{x}—Ni2—Ni2^{vi}	102.914 (14)
Ni1^{viii}—Ge2—Ni2	116.398 (15)	Ni2^{ii}—Ni2—Ni2^{vi}	90.0
Ni1^{ix}—Ge2—Ni2	63.602 (15)	Ge1—Ni2—Ni2^{iv}	54.7
Ni1^{x}—Ge2—Ni2	63.602 (15)	Ge2^{xvii}—Ni2—Ni2^{iv}	57.451 (17)
Ni1^{xi}—Ge2—Ni2	116.398 (15)	Ge2—Ni2—Ni2^{iv}	126.587 (8)
Ni2^{ii}—Ge2—Ni2	65.10 (3)	Ge2^{xv}—Ni2—Ni2^{iv}	126.587 (8)
Ni2^{xii}—Ge2—Ni2	114.90 (3)	Ni1^{ix}—Ni2—Ni2^{iv}	102.914 (14)
Ni2^{xiii}—Ge2—Ni2	180.0	Ni1^{xii}—Ni2—Ni2^{iv}	102.914 (14)
Ni1^{viii}—Ge2—Ge^{xiv}	117.61 (2)	Ni1^{x}—Ni2—Ni2^{iv}	161.57 (2)
Ni1^{ix}—Ge2—Ge^{xiv}	62.39 (2)	Ni2^{ii}—Ni2—Ni2^{iv}	90.0
Ni1^{x}—Ge2—Ge^{xiv}	117.61 (2)	Ni2^{vi}—Ni2—Ni2^{iv}	90.0
Ni1^{xi}—Ge2—Ge^{xiv}	62.39 (2)	Ge1—Ni2—Ge^{xvii}	81.85 (4)
Ni2^{ii}—Ge2—Ge^{xiv}	118.60 (4)	Ge2^{xvii}—Ni2—Ge^{xvii}	165.96 (5)
Ni2^{xii}—Ge2—Ge^{xiv}	61.40 (4)	Ge2—Ni2—Ge^{xvii}	66.123 (16)
Ni2^{xiii}—Ge2—Ge^{xiv}	61.40 (4)	Ge2^{xv}—Ni2—Ge^{xvii}	66.123 (16)
Ni2—Ge2—Ge^{xiv}	118.60 (4)	Ni1^{ix}—Ni2—Ge^{xvii}	114.04 (3)
Ni1^{viii}—Ge2—Mg^{xv}	117.61 (2)	Ni1^{xii}—Ni2—Ge^{xvii}	114.04 (3)
Ni1^{ix}—Ge2—Mg^{xv}	62.39 (2)	Ni1^{x}—Ni2—Ge^{xvii}	61.84 (4)
Ni1^{x}—Ge2—Mg^{xv}	117.61 (2)	Ni2^{ii}—Ni2—Ge^{xvii}	60.92 (2)
Ni1^{xi}—Ge2—Mg^{xv}	62.39 (2)	Ni2^{vi}—Ni2—Ge^{xvii}	60.92 (2)
Ni2^{ii}—Ge2—Mg^{xv}	61.40 (4)	Ni2^{iv}—Ni2—Ge^{xvii}	136.59 (4)
Ni2^{xii}—Ge2—Mg^{xv}	118.60 (4)	Ge1—Ni2—Ge^{xv}	81.85 (4)
Ni2^{xiii}—Ge2—Mg^{xv}	118.60 (4)	Ge2^{xvii}—Ni2—Ge^{xv}	66.123 (16)
Ni2—Ge2—Mg^{xv}	61.40 (4)	Ge2—Ni2—Ge^{xv}	66.123 (16)
Ge^{xiv}—Ge2—Mg^{xv}	69.2	Ge2^{xv}—Ni2—Ge^{xv}	165.96 (5)
Ni1^{viii}—Ge2—Mg^{xvi}	62.39 (2)	Ni1^{ix}—Ni2—Ge^{xv}	61.84 (4)
Ni1^{ix}—Ge2—Mg^{xvi}	117.61 (2)	Ni1^{xii}—Ni2—Ge^{xv}	114.04 (3)
Ni1^{x}—Ge2—Mg^{xvi}	62.39 (2)	Ni1^{x}—Ni2—Ge^{xv}	114.04 (3)
Ni1^{xi}—Ge2—Mg^{xvi}	117.61 (2)	Ni2^{ii}—Ni2—Ge^{xv}	60.92 (2)
Ni2^{ii}—Ge2—Mg^{xvi}	118.60 (4)	Ni2^{vi}—Ni2—Ge^{xv}	136.59 (4)
Ni2^{xii}—Ge2—Mg^{xvi}	61.40 (4)	Ni2^{iv}—Ni2—Ge^{xv}	60.92 (2)
Ni2^{xiii}—Ge2—Mg^{xvi}	61.40 (4)	Ge^{xvii}—Ni2—Ge^{xv}	118.025 (17)
Ni2—Ge2—Mg^{xvi}	118.60 (4)	Ni1^{xii}—Mg—Ni1^{xxiii}	163.12 (10)
Ge^{xiv}—Ge2—Mg^{xvi}	110.8	Ni1^{xii}—Mg—Ni1^{xxiv}	88.766 (14)
Mg^{xv}—Ge2—Mg^{xvi}	180.0	Ni1^{xxiii}—Mg—Ni1^{xxiv}	88.766 (14)
Ni1^{viii}—Ge2—Mg^{xvii}	62.39 (2)	Ni1^{xii}—Mg—Ni1^{xxv}	88.766 (14)
Ni1^{ix}—Ge2—Mg^{xvii}	117.61 (2)	Ni1^{xxiii}—Mg—Ni1^{xxv}	88.766 (14)
Ni1^{x}—Ge2—Mg^{xvii}	62.39 (2)	Ni1^{xxiv}—Mg—Ni1^{xxv}	163.12 (10)
Ni1^{xi}—Ge2—Mg^{xvii}	117.61 (2)	Ni1^{xii}—Mg—Ni2	55.03 (2)
Ni2^{ii}—Ge2—Mg^{xvii}	61.40 (4)	Ni1^{xxiii}—Mg—Ni2	141.85 (8)
Ni2^{xii}—Ge2—Mg^{xvii}	118.60 (4)	Ni1^{xxiv}—Mg—Ni2	96.12 (3)
Ni2^{xiii}—Ge2—Mg^{xvii}	118.60 (4)	Ni1^{xxv}—Mg—Ni2	96.12 (3)
Ni2—Ge2—Mg^{xvii}	61.40 (4)	Ni1^{xii}—Mg—Ni2^{vii}	141.85 (8)
Ge^{xiv}—Ge2—Mg^{xvii}	180.0	Ni1^{xxiii}—Mg—Ni2^{vii}	55.03 (2)
Mg^{xv}—Ge2—Mg^{xvii}	110.80 (9)	Ni1^{xxiv}—Mg—Ni2^{vii}	96.12 (3)
Mg^{xvi}—Ge2—Mg^{xvii}	69.20 (9)	Ni1^{xxv}—Mg—Ni2^{vii}	96.12 (3)

Ge2^{xviii}—Ni1—Ge2^{x}	119.970 (1)	Ni2—Mg—Ni2^{vii}	86.83 (7)
Ge2^{xviii}—Ni1—Ge2^{xix}	119.970 (1)	Ni1^{xii}—Mg—Ni2^{vi}	96.12 (3)
Ge2^{x}—Ni1—Ge2^{xix}	119.970 (1)	Ni1^{xxiii}—Mg—Ni2^{vi}	96.12 (3)
Ge2^{xviii}—Ni1—Ni2^{x}	164.15 (4)	Ni1^{xxiv}—Mg—Ni2^{vi}	141.85 (8)
Ge2^{x}—Ni1—Ni2^{x}	61.740 (4)	Ni1^{xxv}—Mg—Ni2^{vi}	55.03 (2)
Ge2^{xix}—Ni1—Ni2^{x}	61.740 (4)	Ni2—Mg—Ni2^{vi}	58.15 (4)
Ge2^{xviii}—Ni1—Ni2^{xii}	61.740 (4)	Ni2^{vii}—Mg—Ni2^{vi}	58.15 (4)
Ge2^{x}—Ni1—Ni2^{xii}	164.15 (4)	Ni1^{xii}—Mg—Ni2^{iv}	96.12 (3)
Ge2^{xix}—Ni1—Ni2^{xii}	61.740 (4)	Ni1^{xxiii}—Mg—Ni2^{iv}	96.12 (3)
Ni2^{x}—Ni1—Ni2^{xii}	111.970 (18)	Ni1^{xxiv}—Mg—Ni2^{iv}	55.03 (2)
Ge2^{xviii}—Ni1—Ni2^{ix}	61.740 (4)	Ni1^{xxv}—Mg—Ni2^{iv}	141.85 (8)
Ge2^{x}—Ni1—Ni2^{ix}	61.740 (4)	Ni2—Mg—Ni2^{iv}	58.15 (4)
Ge2^{xix}—Ni1—Ni2^{ix}	164.15 (4)	Ni2^{vii}—Mg—Ni2^{iv}	58.15 (4)
Ni2^{x}—Ni1—Ni2^{ix}	111.970 (18)	Ni2^{vi}—Mg—Ni2^{iv}	86.83 (7)
Ni2^{xii}—Ni1—Ni2^{ix}	111.970 (18)	Ni1^{xii}—Mg—Ge2^{xxvi}	135.598 (4)
Ge2^{xviii}—Ni1—Ni1^{ix}	107.624 (17)	Ni1^{xxiii}—Mg—Ge2^{xxvi}	48.589 (5)
Ge2^{x}—Ni1—Ni1^{ix}	107.624 (17)	Ni1^{xxiv}—Mg—Ge2^{xxvi}	48.589 (5)
Ge2^{xix}—Ni1—Ni1^{ix}	55.73 (2)	Ni1^{xxv}—Mg—Ge2^{xxvi}	135.598 (4)
Ni2^{x}—Ni1—Ni1^{ix}	59.148 (17)	Ni2—Mg—Ge2^{xxvi}	110.29 (6)
Ni2^{xii}—Ni1—Ni1^{ix}	59.148 (17)	Ni2^{vii}—Mg—Ge2^{xxvi}	52.47 (2)
Ni2^{ix}—Ni1—Ni1^{ix}	108.43 (2)	Ni2^{vi}—Mg—Ge2^{xxvi}	110.29 (6)
Ge2^{xviii}—Ni1—Ni1^{x}	55.73 (2)	Ni2^{iv}—Mg—Ge2^{xxvi}	52.47 (2)
Ge2^{x}—Ni1—Ni1^{x}	107.624 (17)	Ni1^{xii}—Mg—Ge2^{xxvii}	135.598 (4)
Ge2^{xix}—Ni1—Ni1^{x}	107.624 (17)	Ni1^{xxiii}—Mg—Ge2^{xxvii}	48.589 (5)
Ni2^{x}—Ni1—Ni1^{x}	108.43 (2)	Ni1^{xxiv}—Mg—Ge2^{xxvii}	135.598 (4)
Ni2^{xii}—Ni1—Ni1^{x}	59.148 (17)	Ni1^{xxv}—Mg—Ge2^{xxvii}	48.589 (5)
Ni2^{ix}—Ni1—Ni1^{x}	59.148 (17)	Ni2—Mg—Ge2^{xxvii}	110.29 (6)
Ni1^{ix}—Ni1—Ni1^{x}	60.0	Ni2^{vii}—Mg—Ge2^{xxvii}	52.47 (2)
Ge2^{xviii}—Ni1—Ni1^{xii}	107.624 (17)	Ni2^{vi}—Mg—Ge2^{xxvii}	52.47 (2)
Ge2^{x}—Ni1—Ni1^{xii}	55.73 (2)	Ni2^{iv}—Mg—Ge2^{xxvii}	110.29 (6)
Ge2^{xix}—Ni1—Ni1^{xii}	107.624 (17)	Ge2^{xxvi}—Mg—Ge2^{xxvii}	88.132 (16)
Ni2^{x}—Ni1—Ni1^{xii}	59.148 (17)	Ni1^{xii}—Mg—Ge2^{xv}	48.589 (5)
Ni2^{xii}—Ni1—Ni1^{xii}	108.43 (2)	Ni1^{xxiii}—Mg—Ge2^{xv}	135.598 (4)
Ni2^{ix}—Ni1—Ni1^{xii}	59.148 (17)	Ni1^{xxiv}—Mg—Ge2^{xv}	135.598 (4)
Ni1^{ix}—Ni1—Ni1^{xii}	60.0	Ni1^{xxv}—Mg—Ge2^{xv}	48.589 (5)
Ni1^{x}—Ni1—Ni1^{xii}	60.0	Ni2—Mg—Ge2^{xv}	52.47 (2)
Ge2^{xviii}—Ni1—Ge^{xx}	132.71 (6)	Ni2^{vii}—Mg—Ge2^{xv}	110.29 (6)
Ge2^{x}—Ni1—Ge^{xx}	69.03 (2)	Ni2^{vi}—Mg—Ge2^{xv}	52.47 (2)
Ge2^{xix}—Ni1—Ge^{xx}	69.03 (2)	Ni2^{iv}—Mg—Ge2^{xv}	110.29 (6)
Ni2^{x}—Ni1—Ge^{xx}	63.13 (5)	Ge2^{xxvi}—Mg—Ge2^{xv}	159.20 (9)
Ni2^{xii}—Ni1—Ge^{xx}	122.689 (18)	Ge2^{xxvii}—Mg—Ge2^{xv}	88.132 (16)
Ni2^{ix}—Ni1—Ge^{xx}	122.689 (18)	Ni1^{xii}—Mg—Ge2^{xvii}	48.589 (5)
Ni1^{ix}—Ni1—Ge^{xx}	113.00 (4)	Ni1^{xxiii}—Mg—Ge2^{xvii}	135.598 (4)
Ni1^{x}—Ni1—Ge^{xx}	171.56 (5)	Ni1^{xxiv}—Mg—Ge2^{xvii}	48.589 (5)
Ni1^{xii}—Ni1—Ge^{xx}	113.00 (4)	Ni1^{xxv}—Mg—Ge2^{xvii}	135.598 (4)
Ge2^{xviii}—Ni1—Mg^{xxi}	69.03 (2)	Ni2—Mg—Ge2^{xvii}	52.47 (2)
Ge2^{x}—Ni1—Mg^{xxi}	132.71 (6)	Ni2^{vii}—Mg—Ge2^{xvii}	110.29 (6)
Ge2^{xix}—Ni1—Mg^{xxi}	69.03 (2)	Ni2^{vi}—Mg—Ge2^{xvii}	110.29 (6)

Ni2^{x}—Ni1—Mg^{xxi}	122.689 (18)	Ni2^{iv}—Mg—Ge2^{xvii}	52.47 (2)
Ni2^{xii}—Ni1—Mg^{xxi}	63.13 (5)	Ge2^{xxvi}—Mg—Ge2^{xvii}	88.132 (16)
Ni2^{ix}—Ni1—Mg^{xxi}	122.689 (18)	Ge2^{xxvii}—Mg—Ge2^{xvii}	159.20 (9)
Ni1^{ix}—Ni1—Mg^{xxi}	113.00 (4)	Ge2^{xv}—Mg—Ge2^{xvii}	88.132 (16)

Symmetry codes: (i) −*x*, −*y*, −*z*; (ii) −*x*, *y*, *z*; (iii) −*x*, −*y*, *z*; (iv) *x*, *y*, −*z*; (v) −*x*, *y*, −*z*; (vi) *x*, −*y*, *z*; (vii) *x*, −*y*, −*z*; (viii) *x*−1/2, −*y*+1/2, *z*; (ix) −*x*+1/2, *y*, −*z*+1/2; (x) −*x*+1/2, −*y*+1/2, *z*; (xi) *x*−1/2, *y*, −*z*+1/2; (xii) *x*, −*y*+1/2, −*z*+1/2; (xiii) −*x*, −*y*+1/2, −*z*+1/2; (xiv) −*y*, −*z*+1/2, −*x*+1/2; (xv) *z*, *x*, *y*; (xvi) −*z*, −*x*+1/2, −*y*+1/2; (xvii) *y*, *z*, *x*; (xviii) −*y*+1/2, *z*, −*x*+1/2; (xix) *z*, −*x*+1/2, −*y*+1/2; (xx) *y*+1/2, *z*+1/2, *x*; (xxi) *x*, *y*+1/2, *z*+1/2; (xxii) *z*+1/2, *x*, *y*+1/2; (xxiii) *x*, *y*−1/2, *z*−1/2; (xxiv) *x*, −*y*+1/2, *z*−1/2; (xxv) *x*, *y*−1/2, −*z*+1/2; (xxvi) *z*, −*x*, −*y*; (xxvii) −*y*+1/2, *z*−1/2, −*x*.